
**Submission code: 5RQDMZ09G9**

See this and other abstracts on our website: https://home.sbgf.org.br/Pages/resumos.php

# A Mechanics-Based Advection–Diffusion Framework for Localized Quasi-Static Granular Flow in Random Packings.

**Rodolfo Morales Gálvez (Universidad de Chile), Aldo Tamburrino (Universidad de Chile)**

**A Mechanics-Based Advection–Diffusion Framework for Localized Quasi-Static Granular Flow in Random Packings**

Please, do not insert author names in your submission PDF file.



# Introduction

Granular materials continue to challenge unified theoretical descriptions across arbitrary geometries and loading conditions, frequently exhibiting behaviors that elude classical continuum mechanics. Typical examples include the ellipsoidal-shaped flow core observed during silo discharge and the finite-thickness shear layers that form on inclined planes and in annular Couette cells. These zones have characteristic thicknesses of only a few grain diameters, prompting the widespread use of advection–diffusion–type models to reproduce the measured velocity profiles.

Beginning with Litwiniszyn's random-walk picture for silo drainage in the late 1950s, researchers have turned to stochastic descriptions in which the ensemble behavior of particles, voids, or "bubbles" of free volume evolves by coupled advection–diffusion processes. The void-diffusion and kinematic models of Mullins (1972) and Nedderman Tüzün (1979) reproduce many velocity profiles but overpredict particle mixing and require an empirically expanding diffusion length. Later refinements, notably Bazant's bubble-propagation framework and the Stochastic Flow Rule (SRF) of Kamrin Bazant (2007), added nonlocal drift tied to granular failure criteria, capturing flow-zone thicknesses across silos, inclined planes, and Couette geometries. Yet these treatments remain phenomenological: the advection–diffusion form is assumed rather than derived from first principles, and predictive power hinges on fitted parameters with no direct mechanical interpretation.

Here we derive such governing equations directly from mechanical principles and show that the extent of the flowing zone is controlled by a previously unrecognized dimensionless group: the ratio of driving to resisting forces acting on clusters of mobilized particles. Closed-form analytical solutions and high-resolution numerical simulations are presented, and the model's predictions are benchmarked against published data sets for silo discharge (Fullard et al., 2019), inclined-plane flow (Wang et al., 2019), and annular Couette shear (Mueth et al., 2000; Bocquet et al., 2002; Cruz, 2004). In every case the theory captures both the shape and thickness of the flowing region without parameter tuning, demonstrating that the proposed dimensionless number governs regime transitions in quasi-static granular flow. The framework therefore provides a unified, mechanics-based tool for anticipating flow localization in randomly packed granular media under diverse boundary conditions.

# Proposed theoretical model

Quasi-static granular flow involves correlated clusters of grains whose internal interactions occur at the particle scale while their collective motion spans many diameters. To bridge these scales we invoke the *volume–averaging theorem*: any balance law written for the microscopic fields can be integrated over a control volume that moves with the flowing cluster and then decomposed into a bulk (volume) term plus a boundary (surface) term. Applied to the grain-scale momentum equation, this procedure yields a macroscopic balance in which the divergence of the *averaged* stress tensor is *not* the only source of momentum change. A second contribution, expressible as a surface integral of the fluctuating tractions that act on the boundary of the control volume, appears naturally. We interpret this additional term as an *effective friction force*: it captures the net resistance generated when the fluidized cluster shears against its more static surroundings, and it vanishes when relative motion ceases.

The remainder of this chapter formalizes the averaging operation, derives the explicit form of the surface contribution, and shows how the resulting friction term converts the averaged momentum equation into an advection–diffusion–type law whose transport coefficients are fixed by micro-mechanical parameters.

**1. Volume averaging:** For any microscopic field $B(\mathbf{x}', t)$ defined on the solid phase of a control volume $V$ that encloses a correlated cluster of moving grains, we use the intrinsic average

$$\langle B \rangle_s(\mathbf{x}, t) = \frac{1}{V_s} \int_{V_s} B(\mathbf{x}', t)\, dV_s \tag{1}$$

with the relation to the superficial average

$$\langle B \rangle = \phi_s \, \langle B \rangle_s, \qquad \phi_s = \frac{V_s}{V}. \tag{2}$$

**2. From the microscopic to the macroscopic momentum balance:** Starting from the grain-scale balance

$$\rho\big(\partial_t + u_j \partial_j\big) u_i = \partial_j \sigma_{ij} - \rho g_i, \tag{3}$$

volume-averaging gives

$$\rho\big(\partial_t + \langle u_j \rangle_s \partial_j\big) \langle u_i \rangle_s = \partial_j \langle \sigma_{ij} \rangle_s - \rho g_i - f_i, \tag{4}$$

where the *effective surface force*

$$f_i = \partial_j \langle \sigma_{ij} \rangle_s - \langle \partial_j \sigma_{ij} \rangle_s \tag{5}$$

captures boundary shear lost during coarse-graining.

**3. Physical interpretation of $f_i$:** Write the stress field as

$$\sigma_{ij} = \langle \sigma_{ij} \rangle_s + \Delta\sigma_{ij} + \delta\sigma_{ij}. \tag{6}$$

The fluctuating parts $\Delta\sigma_{ij}$ (hydrostatic) and $\delta\sigma_{ij}$ (deviatoric) average to zero but generate $f_i$ through their gradients, acting as a Coulomb-type friction that vanishes when relative motion ceases.

**4. Constitutive closure (quasi-static clusters):** Assuming a Bingham-like rheology with friction coefficient $\mu$ and kinematic viscosity $\nu$,

$$\langle \delta\sigma_{ij} \rangle_s = \frac{\mu \langle P \rangle_s}{\langle \dot{\gamma} \rangle_s} \langle \dot{\gamma}_{ij} \rangle_s + \nu\rho \, \langle \dot{\gamma}_{ij} \rangle_s, \quad \delta\sigma \geq \mu \langle P \rangle_s. \tag{7}$$

Eliminating $\langle\dot{\gamma}\rangle_s$ yields a drag law

$$f_i = -\frac{K}{\chi}\, v_i, \tag{8}$$

with

$$\chi = \Big(1 - Y_0 Y\Big)^2, \qquad Y = \frac{D\,\|f\|}{\mu P}. \tag{9}$$

**5. Macroscopic equation of motion for quasi-static flow:** Combining (4) and (8), and separating rigid translation $U_i$ from the internal velocity $v_i$,

$$\rho\big(\partial_t + \langle u_j\rangle_s \partial_j\big)\langle u_i\rangle_s = \partial_j\langle\sigma_{ij}\rangle_s - \rho g_i - \frac{K}{\chi}\, v_i \tag{10}$$

forms the *effective granular motion equation.* In the quasi-static limit, inertia is negligible; the balance reduces to gravity, mean stress gradients, and the frictional drag (8), giving a mechanics-based advection–diffusion structure governed by the single dimensionless parameter $Y$.

## Results and conclusions

For flow down an inclined plane the condition $Y \geq Y_0$ becomes

$$Y \;=\; \frac{D_{50}\,|\partial_y \tau_{xy} - \rho g \sin\theta|}{\mu P} \;=\; \frac{D_{50}\,|\tan\theta - \mu|}{\mu y} \;\geq\; Y_0. \tag{11}$$

Defining the characteristic thickness

$$\delta_y \;\equiv\; \frac{D_{50}\,|\tan\theta - \mu|}{Y_0\,\mu}, \tag{12}$$

we find that motion is confined to $y \leq \delta_y$; the model therefore predicts a flowing-layer thickness equal to $\delta_y$. For steady conditions the velocity profile follows

$$u \;=\; \frac{D_{50}^2}{32\rho\, Y_0^2\,\nu}\,\chi\big(\partial_y\tau_{xy} + \rho g \sin\theta\big) \;=\; \frac{\mu g D_{50}}{32 Y_0 \nu}\cos\theta\,\delta_y\Big(1 - \frac{y}{\delta_y}\Big)^2. \tag{13}$$

For Taylor–Couette shear the criterion $Y \geq Y_0$ reads

$$Y \;=\; \frac{D_{50}}{\mu P}\left|\frac{\partial_r(r^2\tau_{r\theta})}{r^2}\right| \;=\; \frac{2D_{50}}{\mu r}\left|\mu_w - \frac{\mu_w - \mu}{1 - (r_w/\delta_r)^2}\right| \;\geq\; Y_0, \tag{14}$$

so that with

$$\Delta_r \;\equiv\; \delta_r - r_w \;\approx\; \frac{D_{50}(\mu_w - \mu)}{Y_0\,\mu'}\Big(1 + \frac{2D_{50}\mu}{r_w Y_0 \mu'}\Big)^{-1}, \tag{15}$$

flow occurs only for $r \geq r_w + \Delta_r$; $\Delta_r$ is the flowing-layer thickness. The resulting tangential velocity profile is

$$u_\theta \;=\; \frac{D_{50}^2}{32\rho\, Y_0^2\,\nu}\,\frac{\partial_r(r^2\tau_{r\theta})}{r^2}\,\chi \;=\; \frac{\mu P D_{50}}{32\rho\, Y_0 \nu}\,\frac{\delta_r}{r}\,\Big(1 - \frac{r}{\delta_r}\Big)^2. \tag{16}$$

Model predictions are compared with the inclined-plane data of Wang et al. (2019), obtained via Particle Tracking Velocimetry (PTV). The experimental setup consisted of a long, narrow channel (Fig. 1a) with an upper hopper that supplies particles and a lower section inclined $20^\circ$ below the material repose angle. Figure 1b shows excellent agreement between the measured velocity profiles (symbols) and the present model (solid line).

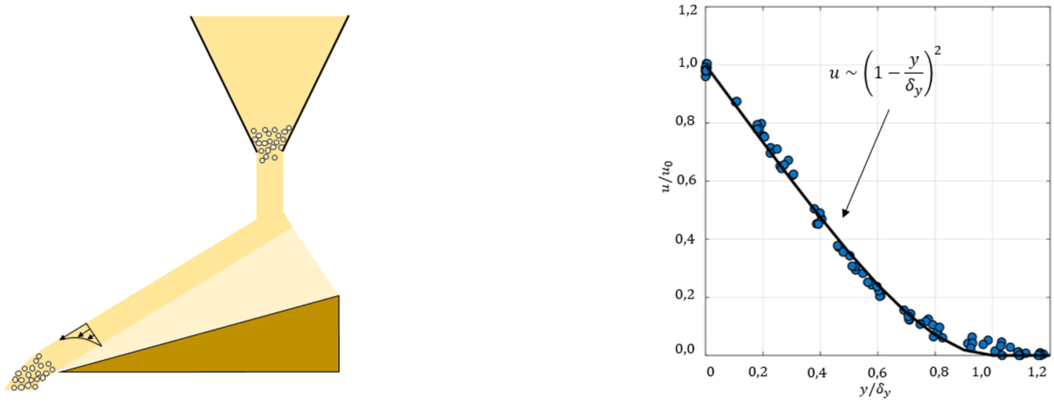


Figure 1: Inclined-plane flow. (a) Experimental apparatus of Wang *et al.* (2019). (b) Horizontal velocity profiles: PTV data (symbols) versus present model (solid line).

Taylor–Couette predictions are assessed against the data compilation of MiDi (2004), which combines the measurements of Mueth et al. (2000), Bocquet et al. (2002), and da Cruz (2004). Figure 2b compares the normalized tangential velocity profiles, again showing close correspondence between theory and experiment.

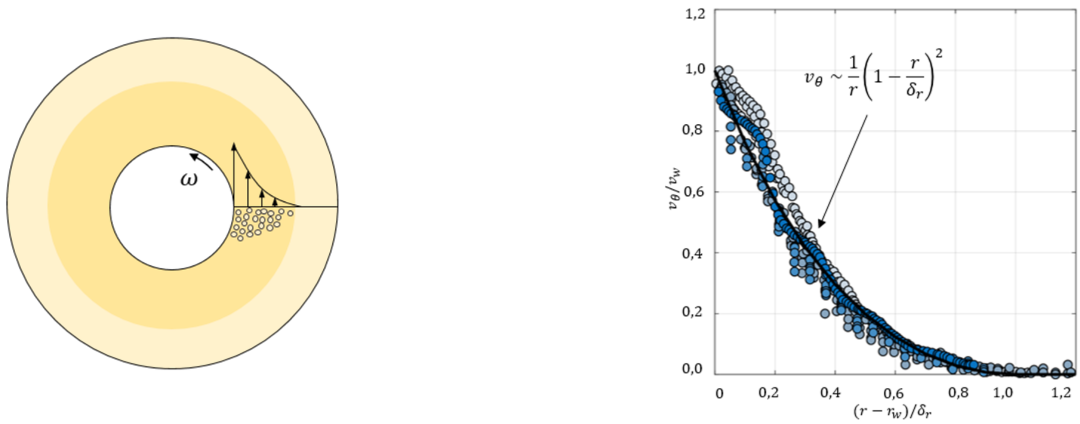


Figure 2: Taylor–Couette flow. (a) Experimental configuration from the MiDi (2004) data set. (b) Normalized tangential velocities: experimental points versus present model (solid line).

For silo discharge the model is implemented in COMSOL MULTIPHYSICS and compared with the Particle Image Velocimetry (PIV) measurements of Fullard et al. (2019). The rectangular silo ($W = 200$ mm, $H = 350$ mm, $D = 15$ mm) contained one or two basal openings of diameter $D_0 = 14$ mm, spaced at various separations $L$. Figure 3b-c shows stationary velocity fields and profiles for the single-orifice case, demonstrating that the proposed model outperforms traditional diffusion-type approaches.

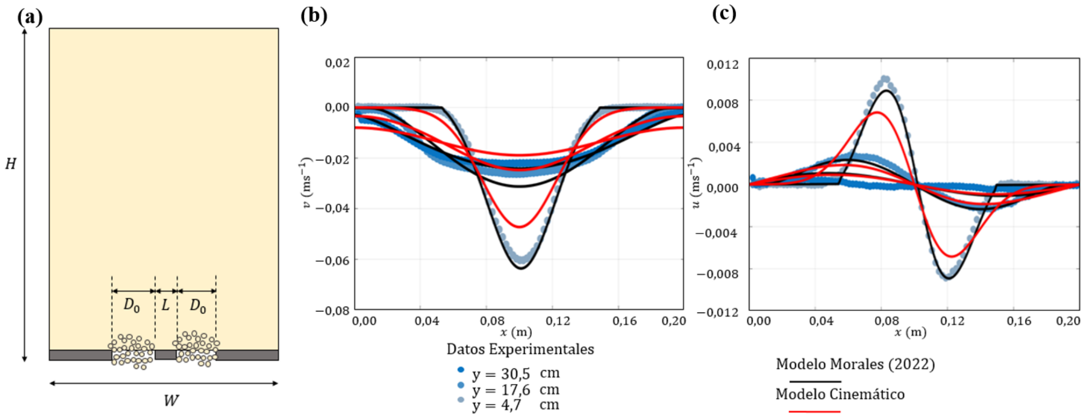


Figure 3: Silo discharge. (a) Experimental geometry (Fullard *et al.*, 2019). (b) Vertical and (c) horizontal velocity profiles at heights 4.7, 17.6, and 30.5 cm: PIV data (symbols) versus present model (solid line).

Overall, the proposed framework reproduces the key features of the flowing zones in all three geometries—inclined plane, Taylor–Couette, and silo discharge—capturing velocity profiles with no additional parameter tuning and thereby underscoring its versatility across distinct stress conditions.

# References

Bocquet, L., W. Losert, D. Schalk, T. Lubensky, and J. Gollub, 2002, Granular shear flow dynamics and forces : Experiment and continuum theory: Physical review. E, Statistical, nonlinear, and soft matter physics, **65**, 011307.

da Cruz, F., 2004, Friction and jamming in granular flows: PhD thesis, Ecole Na- tionale des Ponts et Chaussees, Marne a la vall ee, Franc.

Fullard, L. A., E. C. P. Breard, C. E. Davies, A. J. R. Godfrey, M. Fukuoka, A. Wade, J. Dufek, and G. Lube, 2019, The dynamics of granular flow from a silo with two symmetric openings: Proceedings of the Royal Society A: Mathematical, Physical and Engineering Sciences, **475**, 20180462.

MiDi, G., 2004, On dense granular flows: The European Physical Journal E, **14**, 341–365.

Mueth, D., G. Debregeas, G. Karczmar, P. Eng, S. Nagel, and H. Jaeger, 2000, Signatures of granular microstructure in dense shear flows: Nature, **406**, 385–9.

Wang, N., H. Lu, J. Xu, X. Guo, and H. Liu, 2019, Velocity profiles of granular flows down an inclined channel: International Journal of Multiphase Flow, **110**, 96–107.